Narrow Band Radiative Solutions within a Cubical Enclosure Filled with Real Gas Mixtures

Won-Hee Park
Graduate student, Mechanical Engineering, Chung-Ang University, 221, Huksuk-dong, Dongjak-gu, Seoul 156-756, Korea
Tae-Kuk Kim*
Professor, Mechanical Engineering, Chung-Ang University, 221, Huksuk-dong, Dongjak-gu, Seoul 156-756, Korea

Radiative transfer by nongray gas mixtures with nonuniform concentration and temperature profiles is studied by using the statistical narrow-band model and the ray-tracing method with the sufficiently accurate T_{80} quadrature set. Transmittances through the nonhomogeneous gas mixtures are calculated by using the Curtis-Godson approximation. Three different cases with different temperature and concentration profiles are considered to obtain benchmark solutions for the radiative transfer by nongray gas mixtures. The solutions obtained from this study are verified and found to be very well matched with the previous solutions for uniform gas mixtures. The results presented in this paper can be used as benchmark solutions in developing various solution methods for radiative transfer by nongray gas mixtures.

Key Words : Radiative Transfer, Nongray Gas, Ray-Tracing Method, Narrow Band Model, Curtis-Godson Approximation, T_N Quadrature Set, Nonuniform Gas

Nomenclature

a : Absorption coefficient, m^{-1}
F : Blackbody fraction
G : Average intensity, $W/(m^2 \cdot sr)$
I : Radiative intensity, $W/(m^2 \cdot sr)$
L : System dimension, m
M : Total number of the discrete directions ($=8N^2$ for T_N quadrature)
MM : Number of nodes along a path
$\hat{n}$: Unit vector normal to the wall
P : Partial pressure
q_w : Net radiative wall heat flux, W/m^2
s : Location, m
T : Absolute temperature, K
x, y, z : Coordinates, m
w_m : Angular weight for m^{th} discrete direction

* Corresponding Author,
E-mail : kimtk@cau.ac.kr
TEL : +82-2-820-5282; **FAX** : +82-2-814-9476
Professor, Mechanical Engineering, Chung-Ang University, 221, Huksuk-dong, Dongjak-gu, Seoul 156-756, Korea. (Manuscript **Received** October 25, 2001; **Revised** March 14, 2002)

Greeks

μ, ξ, η : x, y, z direction cosines
$\Delta\lambda_i$: Width of the i^{th} band
Δs_m : Distance of the ray in the m^{th} discrete direction
σ : Stefan-Boltzmann constant, 5.67×10^{-8} $W/(\mu m \cdot K^4)$
τ : Transmittance
Ω : Direction

Subscripts

b : Blackbody
bot : Bottom wall
$exact$: Exact solution
i : i^{th} band
L : Lower limit of the band
max : Maximum value
min : Minimum value
N : Order of the quadrature set
p : Estimation point
$side$: Side wall

top : Top wall
u : Upstream point
U : Upper limit of the band
w : Wall
λ : Spectral

Superscripts

$*$: Dimensionless
$-$: Band averaged

1. Introduction

Radiative heat transfer plays a major role in high temperature systems such as furnaces, combustors, boilers etc. Hence accurate estimation of the radiative heat transfer is essential to these systems. For this reason, various solution schemes for the radiative transfer have been proposed. Among them, there are such schemes developed for regular shapes as the zonal method by Hottel (1967), the Monte Carlo method by Howell and Perlmutter (1964), the PN method by Menguc and Viskanta (1985), the flux method by Lockwood and Spalding (1971) and the discrete ordinate method (DOM) by Carson and Lathrop (1968), Fiveland (1984) and Kim and Lee (1988). For irregular systems, finite volume method (FVM) by Raithby and Chui (1990), radiation element method (REM) by Maruyama and Aihara(1997), and discrete ordinate interpolation method (DOIM) (Cheung and Song, 1997; Seo and Kim, 1998; Kim, Seo, Min and Son, 1998) are suggested.

Although there are many solution methods suggested for three-dimensional enclosures, the applicabilities and accuracies of these methods have not yet been fully tested especially for nongray gases. This is because the measured data and/or the benchmark solutions for the three-dimensional nongray gas radiation are very rare in the literature. Difficulties in modeling radiation with nongray gases are related to the fact that the radiative properties and the intensity are strongly wavelength dependent. Therefore, simple spectral averaging method such as gray gas or gray band approximation may lead to inaccurate solutions. The most accurate results using the line-by-line method (Hartmann etc, 1984; Taine, 1983) requires too much computation times even for one-dimensional problems. To reduce heavy load of calculations, radiative properties are averaged over spectral bands which are the basis of the band model. The narrow band model was used for getting exact solutions (Kim, et al., 1991) for one-dimensional systems. Recently Kim et al. (2001) presented some radiative solutions for nongray gases in an enclosure which has uniform temperature and concentration profiles using the narrow band model.

The purpose of this study is to find highly accurate solutions of radiative transfer for a black walled cubical enclosure filled with nongray gas mixtures which have nonuniform temperature and nonhomogeneous concentration profiles. The discrete transfer method by Lockwood and Shah (1981), which is applied by tracing the rays starting from the black walls to the point in the medium and/or on the wall, is used for the solution and the T_N quadrature set by Thurgood et al. (1995) is adopted for determining the discrete directions and the angular weights. The transmittances through the medium with nonuniform temperature and concentration profiles are computed by using the Curtis-Godson method (Godson, 1953).

2. Basic Equations

2.1 Radiative transfer equation

The radiation transfer equation(RTE) along a line of travel from s_u to s_p in a direction Ω for an absorbing medium as shown in Fig. 1 can be written as (Siegel and Howell, 1992; Modest, 1993.)

$$I_{\lambda,p}(s_p,\Omega)=I_{\lambda,u}(s_u,\Omega)\,e^{-\int_{s_u}^{s_p}a_\lambda(s)ds}+\int_{s_u}^{s_p}a_\lambda(s)\cdot I_{\lambda b}(s)\,e^{-\int_{s}^{s_p}a_\lambda(s')ds'}ds \quad (1)$$

where a_λ is the spectral absorption coefficient and $I_{\lambda b}$ is the spectral blackbody intensity of the medium at s. The transmittance from s_u to s_p is defined as

$$\tau_{\lambda,s_u\to s_p}\equiv e^{-\int_{s_u}^{s_p}a_\lambda(s)ds} \quad (2)$$

Then the RTE can be expressed as

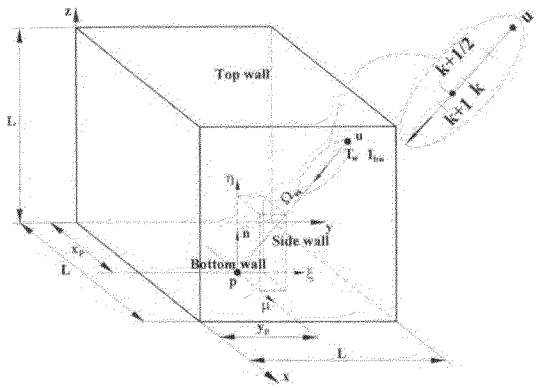

Fig. 1 Schematic drawing of the cubical enclosure

$$I_{\lambda,p}(s_p,\ \Omega)=I_\lambda(s_u,\ \Omega)\,\tau_{\lambda,s_u\to s_p}+\int_{s_u}^{s_p}a_\lambda(s)\,I_{\lambda b}(s)\,\tau_{\lambda,s\to s_p}ds \tag{3}$$

2.2 Narrow band approximation

Since the radiative intensity is a strong function of the wavelength, the RTE needs to be averaged over a finite wavelength interval, $\triangle\lambda$. The procedure of spectral average can be performed for Eq. (3) over $\triangle\lambda$ as

$$\frac{1}{\Delta\lambda}\int_{\lambda_L}^{\lambda_U}[I_{\lambda,p}(s_p,\ \Omega)]\,d\lambda \tag{4}$$

where the narrow band has the lower limit $\lambda_L=\lambda-\Delta\lambda/2$ and upper limit $\lambda_U=\lambda+\Delta\lambda/2$. To simplify notation, the process of averaging over a narrow band will be indicated with the over-bar symbol hereafter. Then the averaged radiative intensity is written as

$$\overline{I}_\lambda=\frac{1}{\Delta\lambda}\int_{\lambda_L}^{\lambda_U}I_\lambda d\lambda \tag{5}$$

Now Eq. (3) becomes

$$\overline{I_{\lambda,p}(s_p,\ \Omega)}=\overline{I_{\lambda,u}(s_u,\ \Omega)\,\tau_{\lambda,s_u\to s_p}}+\int_{s_u}^{s_p}\overline{a_\lambda(s)\,I_{\lambda b}(s)\,\tau_{\lambda,s\to s_p}}ds \tag{6}$$

Since the strong spectral dependencies of the transmittance and the intensity cause correlations between them, the spectral average of their product should be handled carefully. The terms of right hand side of Eq. (6) contain this kind of spectral correlations. However the variation of blackbody intensity with wavelength is relatively smooth as compared to the transmittance, the spectral correlation with the blackbody intensity and the transmittance is negligible (Zhang, et al., 1988; Soufiani and Taine, 1989; Kim et al., 1991). Since all walls are black in this study, upstream point s_u is located on the black wall, the correlation with the blackbody intensity from walls and the transmittance is neglected. Then Eq. (6) can be expressed as

$$\overline{I_{\lambda,p}(s_p,\ \Omega)}=\overline{I_{\lambda,bw}(s_u,\ \Omega)}\cdot\overline{\tau_{\lambda,s_u\to s_p}}+\int_{s_u}^{s_p}\overline{a_\lambda(s)\,\tau_{\lambda,s\to s_p}}\cdot\overline{I_{\lambda b}(s)}\,ds \tag{7}$$

The correlated average, $\overline{a_\lambda(s)\,\tau_{\lambda,s\to s_p}}$, can be expressed explicitly in terms of the transmittance as

$$\overline{\frac{\partial\tau_{\lambda,s\to s_p}}{\partial s}}=\overline{\frac{\partial}{\partial s}\left(e^{-\int_s^{s_p}a_\lambda ds'}\right)}=\overline{a_\lambda(s)\,\tau_{\lambda,s\to s_p}} \tag{8}$$

and we can rewrite Eq. (7) by using the transmittance as

$$\overline{I_{\lambda,p}(s_p,\ \Omega)}=\overline{I_{\lambda,bw}}\cdot\overline{\tau_{\lambda,s_u\to s_p}}+\int_{s_u}^{s_p}\overline{\frac{\partial\tau_{\lambda,s\to s_p}}{\partial s}}\cdot\overline{I_{\lambda b}(s)}\,ds \tag{9a}$$

or by introducing the blackbody fraction as

$$\overline{I_{\lambda,p}(s_p,\ \Omega)}=\frac{\sigma T_w^4}{\pi\Delta\lambda}F_{T_w\lambda_L-T_w\lambda_U}\overline{\tau_{\lambda,s_u\to s_p}}+\int_{s_u}^{s_p}\overline{\frac{\partial\tau_{\lambda,s\to s_p}}{\partial s}}\,\frac{\sigma T_g^4}{\pi\Delta\lambda}F_{T_g\lambda_L-T_g\lambda_U}ds \tag{9b}$$

where the band average radiative intensity $\overline{I}_{\lambda,p}$, the band average transmittance $\overline{\tau}_\lambda$, and the blackbody fraction over the band $F_{T_g\lambda_L-T_g\lambda_U}$ are defined respectively as

$$\overline{I}_{\lambda,p}(s_p,\ \Omega)=\frac{1}{\Delta\lambda}\int_{\lambda_L}^{\lambda_U}I_{\lambda,p}(s,\ \Omega)\,d\lambda \tag{10}$$

$$\overline{\tau}_\lambda=\frac{1}{\Delta\lambda}\int_{\lambda_L}^{\lambda_U}\tau_\lambda(\Delta s)\,d\lambda \tag{11}$$

$$F_{T_g\lambda_L-T_g\lambda_U}=\int_{\lambda_L}^{\lambda_U}\frac{\pi I_{\lambda b}}{\sigma T_g^4}d\lambda \tag{12}$$

Referring to Fig. 1, the path is divided by the MM discrete zones that can be assumed to have uniform temperature and concentration. Then for a discrete direction Ω_m and for a narrow band at λ_i, Eq. (9b) is approximated in the following discrete form as

$$\overline{I_{\lambda i,p,m}}=\frac{\sigma T_w^4}{\pi\Delta\lambda_i}F_{T_w\lambda_{i,L}-T_w\lambda_{i,U}}\overline{\tau_{\lambda,s_U\to s_P}}+\sum_{k=0}^{MM}\left(\overline{\tau_{i,k+1\to MM+1}}-\overline{\tau_{i,k\to MM+1}}\right)\frac{\sigma T_{g,k+1/2}^4}{\pi\Delta\lambda_i}F_{T_{g,k+1/2}\lambda_{i,L}-T_{g,k+1/2}\lambda_{i,U}} \quad (13)$$

where $\Delta\lambda_i$ is the width of the i^{th} band.

By solving Eq. (13), the total radiative intensity at p can then be obtained by simply summing up the intensity for each band as

$$I_{p,m}=\sum_{i=1}^{I}\overline{I}_{i,p,m}\Delta\lambda_i \quad (14)$$

The radiative flux and the averaged radiative intensity are then obtained by using the radiative intensity as

$$q_w^*=\frac{q_w}{\sigma T_{\max}^4}=\frac{1}{\sigma T_{\max}^4}\sum_{m=1}^{M}I_{p,m}(\mu_m \text{ or } \xi_m \text{ or } \eta_m)\,w_m \quad (15)$$

$$G^*=\frac{\pi G}{\sigma T_{\max}^4}=\frac{1}{4\sigma T_{\max}^4}\sum_{m=1}^{M}I_{p,m}w_m \quad (16)$$

where, w_m, μ_m, η_m and ξ_m are the quadrature weight and the x, y, z-direction cosines for the m^{th} ordinate direction which form the T_N quadrature set (Thurgood et al., 1995) where M is the total number of directions. The radiative heat flux from the wall is set positive.

The average transmittance for each narrow band is computed by using the statistical narrow band model (Ludwig, et al., 1973) and the nonisothermal and/or nonhomogeneous gas is treated by using the path averaging procedure called the Curtis-Godson approximation (Godson, 1953). The narrow band parameters from the RADCAL by Grosshandler (1980) are used for the computations over the wave number range between 50cm^{-1} and 9300cm^{-1}.

3. System Descriptions

Numerical calculations are performed for a $L\times L\times L(L=1\text{m})$ cubical enclosure as shown in Fig. 1 where the dimensionless coordinates are defined as $x^*=x/L$, $y^*=y/L$ and $z^*=z/L$. We consider three different cases having different profiles of temperature and concentration. The total pressure of the gas medium is maintained at 1 atm ($P_{CO_2}+P_{H_2O}+P_{N_2}=1\text{atm}$). Maximum temperature, $T_{\max}$, is 1500K and minimum temperature, $T_{\min}$, is 500K.

Case 1 : The medium is a uniform pure CO_2 gas at a uniform temperature. Top wall is maintained at $T_{\max}$ while all other walls and the medium are at $T_{\min}$.

Case 2 : Temperature of the medium and the walls is linearly increased from $T_{\min}$ at the bottom wall to $T_{\max}$ at the top wall along the z-axis. The partial pressure of CO_2 is also linearly increased ($P_{N_2}=0.0$ and $P_{H_2O}=1-P_{CO_2}$.) from the bottom wall.

Case 3 : The medium is a nonuniform mixture of CO_2, H_2O and N_2 as

$$z^*\le z^*_{\max}:\ P_{CO_2}(z^*)=\frac{1}{3}-\left(\frac{z^*_{\max}-z^*}{z^*_{\max}}\right)^2+\frac{2}{3}\left(\frac{z^*_{\max}-z^*}{z^*_{\max}}\right)^3 \quad (17a)$$

$$z^*_{\max}\le z^*\le 1:\ P_{CO_2}(z^*)=\frac{1}{3} \quad (17b)$$

where the partial pressures of H_2O and CO_2 have the relations, $P_{H_2O}=2P_{CO_2}$ and $P_{N_2}=1-P_{CO_2}-P_{H_2O}$, respectively.

The temperature profile is expressed as (Selcuk, 1985)

$z^*\le z^*_{\max}$:

$$T(z^*)=T_{\max}-3(T_{\max}-T_{\min})\left(\frac{z^*_{\max}-z^*}{z^*_{\max}}\right)^2+2(T_{\max}-T_{\min})\left(\frac{z^*_{\max}-z^*}{z^*_{\max}}\right)^3 \quad (18a)$$

$z^*_{\max}\le z^*\le 1$:

$$T(z^*)=T_{\max}-3(T_{\max}-T_e)\left(\frac{z^*-z^*_{\max}}{1-z^*_{\max}}\right)^2+2(T_{\max}-T_e)\left(\frac{z^*-z^*_{\max}}{1-z^*_{\max}}\right)^3 \quad (18b)$$

where $z^*_{\max}$ is the position having the maximum temperature and T_e is the exit temperature at $z^*=1.0$. And in this study these values are $z^*_{\max}=0.5$ and $T_e=1200\text{K}$, respectively. Figure 2 shows the graphical profiles of temperature and partial pressure of CO_2 explained above.

Table 1 Comparison of the current results with the previous ones by Kim, Park and Lee(2001)

x^*	bottom wall heat flux		top wall heat flux		side wall heat flux		average intensity	
	present	Kim et al.	present	Kim et al.	present	Kim et al.	present	Kim et al.
0.00	9.37509E-01	9.37509E-01	1.48265E-01	1.48269E-01	4.68737E-01	4.68747E-01	5.31236E-01	5.31246E-01
0.05	9.37509E-01	9.37509E-01	1.55611E-01	1.55615E-01	3.94059E-01	3.94069E-01	4.53738E-01	4.53024E-01
0.10	9.37509E-01	9.37509E-01	1.63750E-01	1.63754E-01	3.57148E-01	3.57157E-01	4.11710E-01	4.11794E-01
0.15	9.37509E-01	9.37509E-01	1.70777E-01	1.70781E-01	3.23905E-01	3.23913E-01	3.74557E-01	3.74509E-01
0.20	9.37509E-01	9.37509E-01	1.77227E-01	1.77232E-01	2.93115E-01	2.93123E-01	3.41487E-01	3.41119E-01
0.25	9.37509E-01	9.37509E-01	1.83201E-01	1.83206E-01	2.64564E-01	2.64570E-01	3.09803E-01	3.09816E-01
0.30	9.37509E-01	9.37509E-01	1.87733E-01	1.87738E-01	2.38916E-01	2.38922E-01	2.82137E-01	2.82230E-01
0.35	9.37509E-01	9.37509E-01	1.91484E-01	1.91488E-01	2.15210E-01	2.15215E-01	2.58255E-01	2.57611E-01
0.40	9.37509E-01	9.37509E-01	1.94508E-01	1.94428E-01	1.93724E-01	1.93729E-01	2.36246E-01	2.36236E-01
0.45	9.37509E-01	9.37509E-01	1.96096E-01	1.96101E-01	1.74406E-01	1.74410E-01	2.17577E-01	2.17115E-01
0.50	9.37509E-01	9.37509E-01	1.96509E-01	1.96514E-01	1.57062E-01	1.57066E-01	2.03853E-01	2.02546E-01
0.55	9.37509E-01	9.37509E-01	1.96096E-01	1.96101E-01	1.41533E-01	1.41536E-01	1.85990E-01	1.86094E-01
0.60	9.37509E-01	9.37509E-01	1.94508E-01	1.94024E-01	1.27746E-01	1.27749E-01	1.73647E-01	1.73582E-01
0.65	9.37509E-01	9.37509E-01	1.91484E-01	1.91488E-01	1.15236E-01	1.15239E-01	1.62883E-01	1.62743E-01
0.70	9.37509E-01	9.37509E-01	1.87733E-01	1.87738E-01	1.04093E-01	1.04096E-01	1.53072E-01	1.53031E-01
0.75	9.37509E-01	9.37509E-01	1.83201E-01	1.83206E-01	9.41356E-02	9.41380E-02	1.44721E-01	1.44637E-01
0.80	9.37509E-01	9.37509E-01	1.77227E-01	1.77232E-01	8.53385E-02	8.53407E-02	1.37523E-01	1.37317E-01
0.85	9.37509E-01	9.37509E-01	1.70777E-01	1.70781E-01	7.73403E-02	7.73422E-02	1.30489E-01	1.30565E-01
0.90	9.37509E-01	9.37509E-01	1.63750E-01	1.63577E-01	7.02038E-02	7.02056E-02	1.24717E-01	1.24751E-01
0.95	9.37509E-01	9.37509E-01	1.55611E-01	1.55615E-01	6.41308E-02	6.41324E-02	1.20002E-01	1.19751E-01
1.00	9.37509E-01	9.37509E-01	1.48265E-01	1.48269E-01	5.77781E-02	5.77795E-02	1.15068E-01	1.15093E-01
error	0%		0.021%		0.002%		0.104%	

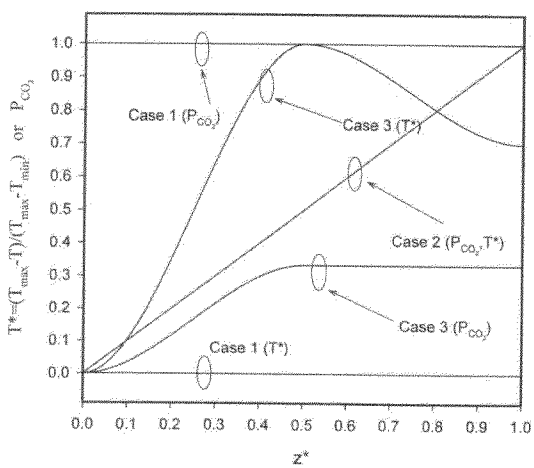

Fig. 2 Profiles of partial pressure of CO_2 and temperature along the z axis

4. Numerical Solutions

In this paper, the radiative heat fluxes are computed on the bottom and top walls along the x axis at $y=0.5L$ and on the side wall along the z axis at $y=0.5L$, respectively. And the average intensities are computed along the z axis through the medium at $x=y=0.5L$. To obtain the numerical solutions with sufficient accuracy, the number of the spatial discretization is set to be $MM=20$ and the number of the angular discretization is set to be $N=60$ ($M=28800$ directions). The typical CPU time is about 230 hours on a Pentium III 733 MHz PC.

4.1 Validation of the results

To validate the solution procedure used in this work, we compare the current result with the previous work by Kim et al. (2001), where the radiative transfer for uniform temperature and concentration(case 1) is analyzed by using the SNB model and ray-tracing method with sufficiently accurate T_{95} quadrature. The black cubical enclosure is filled with the pure CO_2 gas whereas one wall is maintained 1000K and the medium and the other walls are at the temperature of 500K. Table 1 compares the results obtained from this study with the previous one. Relative errors for radiative heat fluxes and average inten-

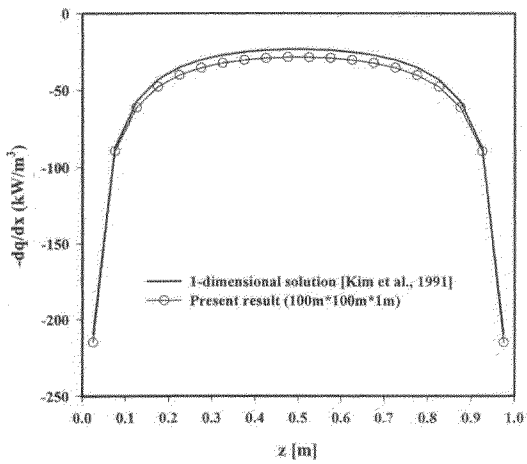

Fig. 3 Comparison of the present result and the result for the infinite plane layer

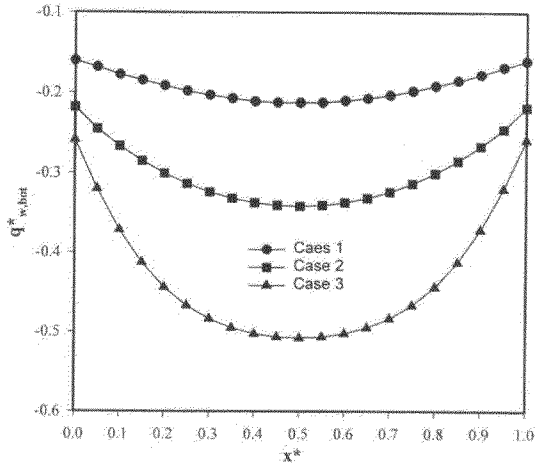

Fig. 4 Net bottom wall heat fluxes ($z^*=0.0$, $y^*=0.5$)

sity are also shown in Table 1. The wall heat fluxes are very well matched with the previous solutions but the errors for the average intensity are appreciable. This shows that the current results obtained by using the Curtis-Godson approximation and the T_{60} quadrature set are accurate enough to be regarded as benchmark solutions.

Another way to show our calculations are appropriate is to compare our results with the previous solutions of the 1-dimensional infinite plane layer problem (Kim, et al. 1991). To compare with the 1-dimensional system, a rectangular system with 100m×100m×1m is considered. The bottom and top walls are maintained at 0K and the other walls and the medium are maintained at 1000K. The medium in the system is the pure H_2O gas at 1 atm. The radiative source terms are obtained along the central z line of the thin rectangle. Figure 3 shows the radiative source terms obtained from the 1-dimensional and the 3-dimensional analyses, respectively. The results agree fairly well with each other, and the differences between the data are possibly due to different SNB models and parameters used for each calculation.

4.2 Solutions by Curtis-Godson approximation

Figure 4 shows dimensionless net wall heat fluxes on the bottom wall ($z^*=0$). The net bottom wall heat fluxes reach a minimum value at the center of x axis in all cases, because the center of bottom wall is most affected by hot medium and hotter walls. But the medium is maintained at $T_{\min}$ in the case 1, the radiative bottom wall heat flux has the smallest one. Since the medium has maximum temperature at $z^*=0.5$ in the case 3, the bottom wall heat flux is larger than those of the other cases. The net bottom wall heat flux in the case 2 has an intermediate distribution of net wall heat flux between the case 1 and 3.

Figure 5 shows the dimensionless net wall heat fluxes on the top wall ($z^*=1$). In the case 1, since the top black wall is maintained at $T_{\max}=1500$K and the other black walls and the medium are maintained cold at $T_g=T_{\min}=1/3\,T_{\max}$, the exact analytic solution for net top wall heat flux can be obtained as

$$q^*_{w,top}=\int_{4\pi} I_p\eta d\Omega/\sigma T^4 = \sigma(T^4_{\max}-T^4_{\min})/\sigma T^4_{\max}=0.987654 \tag{19}$$

The dimensionless net top wall heat flux of 0.987661 as shown in Fig. 5 for the case 1 is quite accurate with a relative error of 0.0007%. In case 3, the maximum temperature is located at the mid-height of the system where the side walls are also at the highest temperature. And the net heat flux at the center of the top wall can be reduced

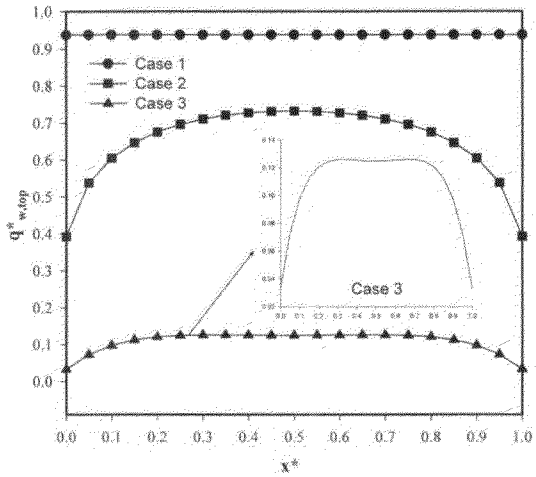

Fig. 5 Net top wall heat fluxes ($z^*=1.0$, $y^*=0.5$)

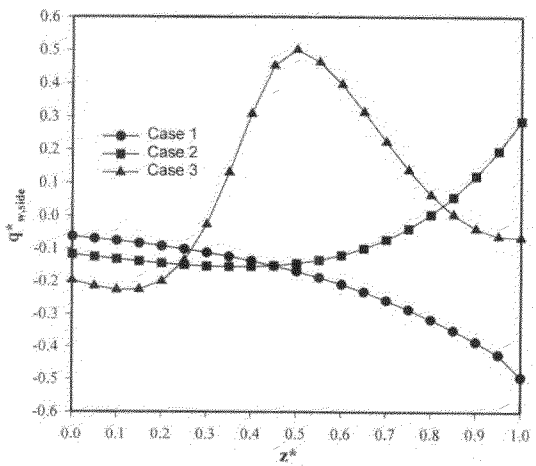

Fig. 6 Net side wall heat fluxes ($x^*=0.5$, $y^*=0.5$)

due to the heat flux from the hottest side wall to the center of the top wall, and this results in the slight drop of the wall heat flux profile shown in Fig. 5 (case 3). The dimensionless net side wall heat fluxes are demonstrated in Fig. 6. The outgoing net side wall flux increases at larger z^* in the case 1 ; the net side wall flux is directed to inside at the smaller z^* and then to outside at the larger z^* in the case 2 ; the net side wall heat flux has the largest at $z^*\approx0.5$ in the case 3.

The dimensionless average intensities along the central z^* axis of the enclosure ($x^*=0.5$, $y^*=0.5$) are given in Fig. 7. Similar to Eq. (19), the exact analytic average intensity on the hot wall can also be obtained as

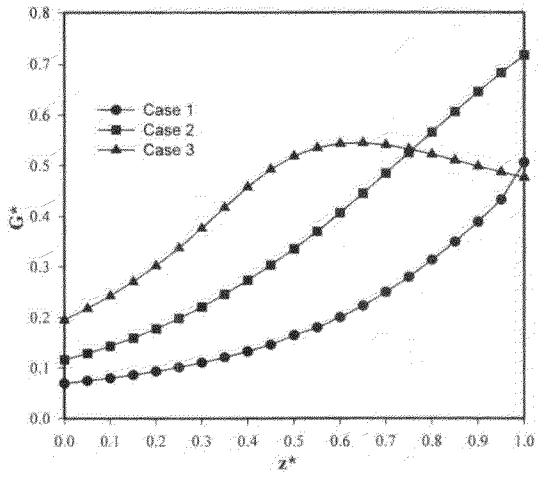

Fig. 7 Average intensities ($x^*=0.5$, $y^*=0.5$)

$$G^*_{w,top}=\frac{1}{4\pi}\int_{4\pi}I_p d\Omega\cdot\pi/\sigma T^4_{\max}$$
$$=\frac{\sigma}{2\pi}(T^4_{\max}+T^4_{\min})\cdot\pi/\sigma T^4_{\max} \quad (20)$$
$$=0.50617$$

The calculated result in the case 1 is 0.50625 as shown in Fig. 6, which is quite accurate with a relative error of 0.016%. In both cases 1 and 2, dimensionless average intensities have a monotonously increasing nature. However, there is a similarity between the profile of the dimensionless average intensity and that of the temperature in the case 3.

5. Conclusion

In this study, the radiative transfer solutions within a cubical enclosure with nonhomogeneous composition and nonuniform temperature profiles are obtained. The nonuniform gas effect is treated by the Curtis-Godson method. The solutions obtained from this study are verified and found to be very well matched with the previous solutions for uniform gas. Three cases are studied in this paper: 1) the medium has uniform temperature and concentration; 2) temperature and concentration of medium have linear profiles; and 3) the profiles of temperature and concentration are

given as a function of z-coordinate by considering a real furnace. In each case, radiative wall heat fluxes and average radiative intensities are obtained. Although the solution method used in this study is not suitable for engineering purposes, the resulting solutions are proved to be quite accurate and can be used as a reference data to verify various schemes for radiative transfer by nongray gases.

Acknowledgment

The authors wish to acknowledge the financial support of the CERC(Combustion Engineering Research Center).

References

Carlson, B. G. and Lathrop, K. D., 1968, "Transport Theory-The Method of Discrete Ordinates," *Computing Methods in Reactor Physics*, Greenspan, H., Kelber, C. N. and Okrent, D. eds., Gordon and breach, New York.

Cheung, K. B. and Song, T. H., 1997, "Discrete Ordinates Interpolation Method for Numerical Solution of Two-Dimensional Radiative Transfer Problems," *Numercial Heat Transfer, Part B*, Vol. 32, pp. 107~125.

Fiveland, W. A., 1984, "Discrete-Ordinates Solutions of the Radiative Transport Equation for Rectangular Enclosures," *ASME Journal of Heat Transfer*, Vol. 106, pp. 699~706.

Godson, W. L., 1953, "The Evaluation of Infrared Radiation Fluxes Due to Atmospheric Water Vapor," *Quarterly Journal of Royal Meteorological Society*, Vol. 79, pp. 367~379.

Grosshandler, W. L., 1980, "Radiative Transfer in Nonhomogeneous Gases : A Simplified Approach," *International Journal of Heat and Mass Transfer*, Vol. 23, pp. 1447~1459.

Hartmann, J. M., Levi Di Leon, R. and Taine, J., 1984, "Line-by-Line and Narrow-Band Statistical Model Calculations for HO," *Journal of Quantitative Spectroscopy and Radiative Transfer*, Vol. 32, No. 2, pp. 119~127.

Hottel, H. C. and Sarofim, A. F., 1967, *Radiative Transfer*, McGraw-Hill.

Howell, J. R. and Perlmutter, M., 1964, "Monte Carlo Solution of Thermal Transfer through Radiant Media Between Gray Walls," *ASME Journal of Heat Transfer*, Vol. 86, No. 1, pp. 116~122.

Kim, T. K. and Lee, H., 1988 "Effect of Anisotropic Scattering on Radiative Heat Transfer in Two-Dimensional Rectangular Enclosures," *International Journal of Heat and Mass Transfer*, Vol. 31, No. 8, pp. 1711~1721.

Kim, T. K., Menart, J. A. and Lee, H., 1991, "Nongray Radiative Gas Analyses Using the S-N Technique," *ASME Journal of Heat Transfer*, Vol. 113, pp. 946~952.

Kim, T. K., Seo, S. H., Min, D. H. and Son, B. S., 1998, "Study on Radiation in 3-D Irregular Systems Using the Trapezoidal Rule Approximation on the Transport Equation," *KSME international Journal*, Vol. 12, No. 3, pp. 514~523.

Kim T. K., Park W. H. and Lee C. H., 2001, "Radiative Transfer Solutions for Purely Absorbing Gray and Nongray Gases within a Cubical Enclosure," *KSME International Journal*, Vol 15, No. 6 pp. 752~763.

Lockwood, F. C. and Spalding, D. B., 1971, "Prediction of a Turbulent Duct Flow with Significant Radiation," *Proc. Thermodynamics Colloquium*.

Lockwood, F. C. and Shah, N. G., 1981, "A New Radiation Solution Method for Incorporation in General Combustion Predictions Procedure," *in 18th Symposium on Combustion, The Combustion Institute, Pittsburg, PA, pp. 1405~1414.*

Ludwig, C. B., Malkmus, W., Readon, J. E. and Thompson, A. L., 1973, Handbook of Infrared Radiation from Combustion Gases, NASA SP-3080, Scientific and Technical Information Office, Washington D.C..

Maruyama S. and Aihara T., 1997, "Radiation Heat Transfer of Arbitrary Three-Dimensional Absorbing, Emitting and Scattering Media and Specular and Diffuse Surfaces," *ASME Journal of Heat Transfer*, Vol. 119, No. 1, pp. 129~136.

Menguc, M. P. and Viskanta, R., 1985, "Radiative Transfer In Three-Dimensional Rectangular

Enclosures Containing Inhomogeneous, Anisotropically Scattering Media," *Journal of Quantitative Spectroscopy and Radiative Transfer*, Vol. 33, No. 6, pp. 533~549.

Modest, M. F., 1993, *Radiative Heat Transfer*, McGraw-Hill, Inc..

Raithby, G. D. and Chui, E. H., 1990, "A Finite-Volume Method for Predicting a Radiant Heat Transfer in Enclosure with Participating Media," *ASME Journal of Heat Transfer*, Vol. 112, pp. 415~423.

Soufiani, A. and Taine, J., 1989, "Experimental and Theoretical Studies of Combined Radiative and Convective Transfer in CO_2 and H_2O Laminar Flows," *International Journal of Heat and Mass Transfer*, Vol. 32, No. 3, pp. 447~486.

Seo, S. H. and Kim, T. K., 1998, "Study on interpolation schemes of the discrete ordinates interpolation method for 3-D Radiative Transfer with Nonorthogonal Grids," *ASME Journal of Heat Transfer*, Vol. 120, pp. 1091~1094.

Siegel, R. and Howell, J. R., 1992, *Thermal Radiation Heat Transfer*, McGraw-Hill Book Co., 3nd Ed.

Taine, J., 1983, "A Line-by-Line Calculation of Low Resolution Radiative Properties of $CO-CO_2$ Transparent Nonisothermal Gas Mixtures up to 3000 K," *Journal of Quantitative Spectroscopy and Radiative Transfer*, Vol. 30, No. 4, pp. 371~379.

Thurgood, C. P., Pollard, A. and Becker, H. A., 1995 "The T_N Quadrature Set for the Discrete Ordinates Method," *ASME Journal of Heat Transfer*, Vol. 117, pp. 1068~1070.

Zhang, L., Soufiani, A. and Taine, J., 1988, "Spectral Correlated and Noncorrelated Radiative Transfer in a Finite Axisymmetric System Containing an Absorbing and Emitting Real Gas-Particle Mixture," *International Journal of Heat and Mass Transfer*, Vol. 31, pp. 2261~2272.